Prepared for submission to JCAP

Are starburst galaxies a common source of high energy neutrinos and cosmic rays?

Cecilia Lunardini,[a] **Gregory S. Vance,**[b] **Kimberly L. Emig,**[c] **Rogier A. Windhorst**[b]

[a]Department of Physics, Arizona State University, Tempe, AZ 85287-1504 USA
[b]School of Earth and Space Exploration, Arizona State University, Tempe, AZ 85287-1404 USA
[c]Leiden Observatory, Leiden University,PO Box 9513, NL-2300 RA Leiden, the Netherlands

E-mail: Cecilia.Lunardini@asu.edu, Gregory.S.Vance@asu.edu, emig@strw.leidenuniv.nl, Rogier.Windhorst@asu.edu

Abstract. A recent analysis of cosmic ray air showers observed at the Pierre Auger Observatory indicates that nearby starburst galaxies (SBGs) might be the cause of $\sim 10\%$ of the Ultra-High-Energy Cosmic Ray flux at energies $E > 39$ EeV. Since high energy neutrinos are a direct product of cosmic ray interactions, we investigate SBGs as a possible source of some of the 0.1-1 PeV neutrinos observed at IceCube. A statistical analysis is performed to establish the degree of positional correlation between the observed neutrinos and a set of nearby, radio- and infrared-bright SBGs. Our results are consistent with no causal correlation. However, a scenario where $\sim 10\%$ of the neutrino data are coming from the candidate SBGs is not excluded. The same conclusion is reached for two different IceCube data sets (and their subsets, including shower-like and track-like events), as well as two different subsets of SBGs motivated by the Pierre Auger Observatory analysis.

Keywords: high energy neutrinos, cosmic rays, star-formation

Contents

1 Introduction

The Ultra-High-Energy Cosmic Rays (UHECR) that the Earth constantly receives from space are the most energetic particles ever observed (see, e.g. [1, 2] for an introduction). They are mainly hadrons (protons and/or atomic nuclei) with energies exceeding the EeV scale [3]. A long-standing goal is to identify the astrophysical sources of the UHECR and, ultimately, understand the acceleration mechanisms that take place there.

In the last five years, cosmic ray physics has entered the multi-messenger era, where cosmic ray and gamma ray data are being complemented by detections of gravitational waves [4] and neutrinos. About 100 neutrinos, with energies $0.1 - 1$ PeV, have been detected by the kilometer-scale experiment IceCube since 2013 [5]. Most of these neutrinos have likely originated from cosmic rays, having been produced in the collision of cosmic rays with ambient protons or photons, either in the sources themselves, or in the medium between the sources and the Earth. Considering that neutrinos propagate unabsorbed and undeflected over cosmological distances, they are ideal probes of the sites and origin of high energy particle acceleration.

Ultimately, the definitive answer to the question of the origin of the UHECR and the high energy neutrinos will be given by an evidence of positional correlation of the observed particles with candidate sources. Therefore, searches for correlations are crucial, and intense multi-messengers searches are ongoing on this front. Recently, an analysis of the data of the Pierre Auger Observatory [6] (we will refer to this paper as AUG from here on) showed an indication of positional correlation of the highest energy cosmic rays with Starburst Galaxies (SBGs), which are characterized by exceptionally high rates of star-formation. Specifically, for the particles with (observed) energies $E > 39$ EeV, a model with 9.7% of the UHECR flux from nearby SBGs (and the remaining 90.3% isotropic) was found to be favored, with 4σ significance, over a completely isotropic scenario. About 90% of the anisotropic flux was found to be attributable to four nearby SBGs: NGC 4945, NGC 253, M83, and NGC 1068. The AUG claim was checked in a new analysis of the Telescope Array (TA) data [7], which gave results consistent with both the AUG anisotropy and with complete isotropy. An independent analysis of the Pierre Auger Observatory data, employing a joint fit of cosmic ray arrival directions and energy spectra, reached conclusions that are broadly consistent with AUG [8].

The Auger/TA results renew the interest in SBGs as possible cosmic ray and neutrino sources. Theoretically, they are well motivated (see e.g., [9, 10]). Indeed, they host episodes

of extremely efficient star-formation, which causes high rates of core collapse supernovae. The resulting supernova ejecta propagate into the interstellar gas, producing shocks where cosmic ray acceleration and neutrino production takes place. Observationally, positional coincidences between the neutrino arrival directions and nearby SBGs were noticed early on [11]. In a statistical analysis, three of us [12] found an excess – although not significant – of coincidences compared to the prediction in absence of a causal relationship. Overall, statistical analyses of coincidences [12–14] constrain the contribution of SBGs to tens of per cent of the total astrophysical neutrino flux, which is in agreement with arguments of consistency between the IceCube data and gamma ray observations [15, 16] (see also [10, 17, 18]). However, the situation of neutrino analyses is still open to including new data, and to including various uncertainties on the consistency argument (see, e.g., [19, 20]). Hence, an update in the light of the AUG result is in order.

In this paper, such an update is presented. There are two main elements of novelty. First, we obtain a new compilation of SBGs that extends the one used in the AUG paper to the southern hemisphere. This is especially important, considering that a large fraction of the neutrino data is located in that part of the sky. Secondly, we use the latest published IceCube data to test for positional associations of the neutrinos with this expanded set of SBGs. The results can be directly compared to those in AUG, and therefore they serve as a natural complement to it, adding one more piece of information to the general multi-messenger landscape. In sec. 2, a description of the method and of the data used is given; our results are presented in sec. 3, followed by a brief discussion in sec. 4. More details on our SBGs compilation are available in Appendix A.

2 Data and methodology

We consider the two most extended sets of IceCube data that are publicly available. The first is the 6-year data set of high-energy starting events (HESE) [21–23], which refers to candidate neutrino detections ("events") for which the neutrino interaction vertex is located inside the fiducial volume of the detector. For each event, the detector gives the topology as track-like (mainly charged-current interactions of muon neutrinos) or shower-like (all other types of interactions), the measured energy and the arrival direction. The latter has a median angular error which is of $\mathcal{O}(1^\circ)$ for track-like and $\mathcal{O}(10^\circ)$ for shower-like events [21–23]. Out of a total of $N_\nu = 79$ HESE events, 58 are shower-like. It is also estimated that $N_b = 40.8^{+18.7}_{-11.2}$ events are due to background (see [23] for details).

The second set is the 6-year list of $N_\nu = 29$ track-like events [24], with their vertex either inside or outside the fiducial volume. For this event sample, the detector field of view is restricted to the Northern Hemisphere.

In the main analysis of AUG (Table 1 in the AUG paper), 23 SBGs are considered. They were obtained by selecting, from a 3-year Fermi-LAT catalog [25], the objects that are closest (distance $d < 250$ Mpc) and brightest (flux density larger than 0.3 Jy at frequency $f = 1.4$ GHz [1]). This list is incomplete in the southern hemisphere (declination $\delta \lesssim -35^\circ$). The authors of AUG examined other SBGs lists as well – specifically those in the Fermi-LAT Third Source Catalog [26] and in the catalog by Becker et al. [27] (see Appendix A) – to further corroborate the anisotropy result, which indeed turned out to be robust. Still,

[1] Throughout this paper, the symbol f will be used for frequency, to be distinguished from ν, the symbol of the neutrino particle. Also, note that 1 Jy $= 10^{-26}\mathrm{Wm}^{-2}\mathrm{Hz}^{-1}$.

however, all of the SBGs lists in AUG were incomplete to some extent, especially in the southern hemisphere[2].

Here we elaborate on the AUG approach of using SBGs from the Becker et al. catalog [27] by extending it to the southern hemisphere. Specifically, the extension was obtained by a two-step process that involved extracting far infra-red observations of galaxies from the IRAS Revised Bright Galaxy sample [31], and combining them with radio data from the Australia-based HI Parkes All Sky Survey [32]. Only sources with radio flux densities larger than 0.3 Jy at $f = 1.4$ GHz (to match the selection of AUG) were included in our final compilation (see Appendix A for more details). The result of this selection process is a set of 45 SBGs, that are listed in Table 1. The set includes the 4 major contributors to the AUG anisotropy, and all but two [3] of the SBGs that appear in Table 1 of AUG. Fig. 1 (left panel) shows the distribution of the candidate sources and of the HESE neutrino data points in the sky, in Equatorial coordinates. The Galactic plane is shown as well.

The statistical analysis is done using a likelihood ratio method, as outlined in [12]. Here the basics of the method will be summarized. For each neutrino data point, i ($i = 1, 2, ..., N_\nu$), the statistical variable of interest is the normalized angular distance to the *closest* candidate source: $r_i = Min_j(S_{ij}/\sigma_i)$. Here, S_{ij} is the angular distance from the neutrino i to the candidate j, and σ_i is the angular error on the neutrino position (the error on the position of SBGs is negligible here). A positional coincidence is defined as $r < 1$ (the index i will be dropped from now on, for brevity). If the candidate sources are indeed a cause of the neutrino flux, the number of coincidences – and, more generally, the number of data points with $r \lesssim 3$ – should be larger than the number expected in the "null case", which is the scenario where the candidate sources are simply distributed uniformly in the sky with no causal connection to the neutrinos. The distribution of r expected in the null case can be calculated either by Monte-Carlo simulation or analytically, as a sum over the neutrino data points (see [12]).

3 Results

The main result of our analysis is shown in fig. 1 (right panel). It presents the distribution of r for the HESE neutrino data and for the null case. The number of observed coincidences is $N_c = 25$, only slightly lower than the prediction in the null hypothesis. The probability (p-value) that a number at least this large is realized in the null case is $p \simeq 0.72$. Overall, the r-distribution is consistent with the one expected in the null case (also shown in fig. 1), leading to the conclusion that there is *no* indication of causal association of the HESE IceCube neutrino data with the nearby SBGs in the considered sample. We checked that a similar degree of consistency with the null case is found when restricting the analysis to the original SBGs list in AUG. Therefore, our conclusion is robust. We also find good agreement with the null case when different bin sizes for the histogram in fig. 1 are used. For example, using a bin size $\Delta r = 0.5$, the number of data points in the first 4 bins are $N = 12, 13, 6, 7$, to be compared with $N \simeq 10.0, 16.5, 13.1, 8.3$ expected in the null hypothesis.

A useful comparison might be with a hypothetical scenario where 10% of the neutrino events is from the candidate sources. These events would cause an excess at $r \lesssim 2$, relative

[2]The situation is expected to vastly improve in the next decade with the new deep multi-color surveys by the Large Synoptic Survey Telescope (LSST) [28] in the South and the all-sky space missions Euclid [29] and WFIRST [30].

[3]The two missing objects are MRK 231 and NGC3556. The former is excluded by our selection criterion on the distance; the latter has flux density below the threshold we have imposed; see the Appendix.

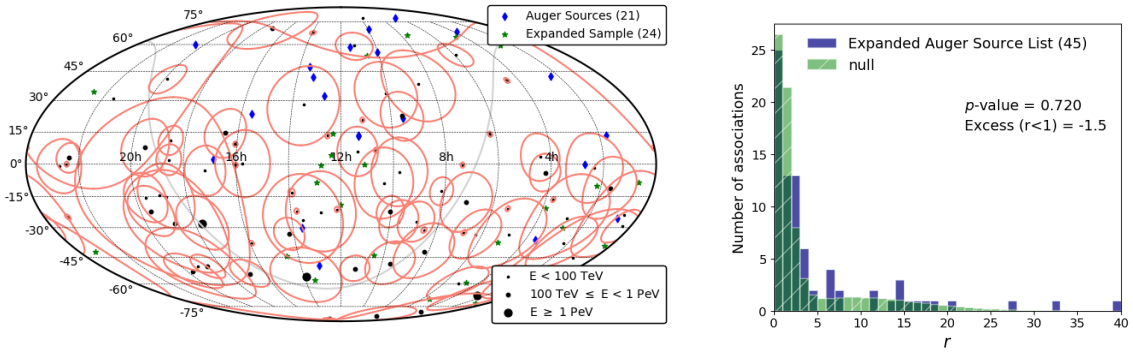

Figure 1. *Left:* Sky map (in J2000 equatorial coordinates) showing the arrival directions of the 6-year set of high-energy starting events (HESE) at the IceCube neutrino observatory (black dots; with dot size indicating bins of observed energy, see legend) with their positional errors (ellipses). Also shown is the set of SBGs considered in the analysis. For these, different markers are used to distinguish the galaxies that appear in the primary analysis of the Pierre Auger collaboration paper (Table 1 in [6]). *Right:* The distribution of the minimum normalized angular distance, r, for the data and for the null case, see Sec. 2.

to the null case. Assuming that this excess is equally distributed between the first two bins, we find that in this case the number of neutrino events with $0 < r \leq 1$ and $1 < r \leq 2$ would be $N_c \simeq 28$ and $N \simeq 23$, respectively, which would be somewhat in tension with the data, but overall consistent with them to within $\sim 3\sigma$ confidence level. Therefore, this scenario is not excluded.

One may wonder if the sensitivity of the analysis suffers from considering a relatively large number of candidate sources, when in fact only 4 objects (in bold in Table 1) were identified in AUG as accounting for most of the observed anisotropy. As a further test, we repeated the analysis using the latter subset. Results are, again, consistent with the null case: taking bins of width $\Delta r = 1$, the number of data points in the first 2 bins are $N = 7, 6$, whereas for the null hypothesis the prediction is $N \simeq 4.2, 9.2$. If 10% of the events were due to the 4 candidate sources, and if they were equally distributed among the first two bins, then the predicted number of neutrino events in those bins would be $N_c \simeq 8$ (for $0 < r \leq 1$) and $N \simeq 12$ (for $1 < r \leq 2$), which are in acceptable agreement with the observed counts, although with some tension in the second bin.

In the same spirit of restricting the investigation to the (potentially) most relevant data, we have also repeated the analyses above for subsets of the neutrino HESE data with higher observed energies: $E_{obs} > 50, 100, 150$ TeV, corresponding to a number of neutrino events $N_\nu = 57, 28, 19$, respectively [4]. Events with higher observed energy might be more likely to be of astrophysical origin, since atmospheric background fluxes are expected to be stronger at lower energy. In all cases, the results are consistent with the null hypothesis.

Let us now discuss the analysis – done with the same method outlined above – for the set of track-like neutrino events from [24] and the SBGs in Table 1. We find zero coincidences, $N_c = 0$. The two minimum values of r are $r = 3.0, 5.7$, for the candidate sources NGC6240 (neutrino event number 6, observed energy $E_{obs} = 770.0$ TeV) and Arp220 (neutrino event

[4]Note how a large neutrino data set where many or most events are background can lead to a situation where the positional error ellipses cover most of the sky (see fig. 1). In this case, one would find a large number of coincidences, that would make a true signal difficult to distinguish.

number 12, $E_{obs} = 300.0$ TeV), respectively. In the null case, the expected number of data points with $r < 6$ is $N \simeq 2$, leading again to the conclusion that the data are consistent with random, non-causal positional association. The 10% hypothesis described above is again disfavored, but not excluded, predicting $N \simeq 3$ in the interval $0 < r \leq 2$, with the observed number ($N = 0$) having a probability $P \simeq 0.05$ of being realized.

4 Discussion and conclusion

To summarize, we find that there is *no* indication of a causal correlation between the neutrino data in the two published IceCube sets and the nearby starburst galaxies considered in AUG. Due to the limited statistics, and to the large errors on the direction of the shower-like neutrino events, a fraction of causally correlated events in the detector at the level of $\sim 10\%$ – which is approximately the size of the effect found in AUG – is marginally allowed by both data sets.

Our result is in agreement with previous multimessenger studies where the contribution of SBGs to the IceCube neutrino data is constrained to be at the level of tens of per cent or less (see, e.g., [15]). More broadly, it is also consistent with two other arguments: (i) the constraints on the neutrino luminosity of certain individual SBGs, obtained from their gamma-ray spectra under naturalness assumptions; and (ii) the fact that, if the neutrino production rate tracks the star-formation rate, most of the detected neutrino flux should be of cosmological origin, with the contribution of nearby ($z < 0.03$) individual sources being only a few per cent at most (or up to a $\sim 10\%$ contribution when relaxing the assumptions on the cosmological evolution of the source population). We refer to [12] for a more extended discussion of these points.

Future analyses with a larger number of neutrino data will be able to further constrain the allowed contribution of nearby SBGs. It is possible that the AUG anisotropy will be established and confirmed to be due to SBGs, and at the same time the neutrino flux from the same sources will be constrained to a much smaller fraction. Such situation could be explained by the neutrino flux being mostly cosmological (whereas the short mean free path of the UHECR suppresses their cosmological flux), as we have discussed. It may also favor scenarios with suppressed pion (and, therefore, neutrino) production efficiency, which can be realized depending on the properties of a galaxy (gas density, galactic wind, etc.), see, e.g., [18] for a discussion.

In conclusion, the question of the role of nearby starburst galaxies in the production of UHECR and neutrinos remains fairly open at this time. It is likely that significant advancements on this front will require disentangling contributions of several classes of objects to the neutrino flux, through extensive multi-year, multi-messenger campaigns that will lead us into the next decade.

Acknowledgments

CL is grateful to Lorenzo Perrone for useful discussions. She acknowledges funding from the National Science Foundation grant number PHY-1613708. KLE acknowledges financial support from the Netherlands Organization for Scientific Research (NWO) through TOP grant 614.001.351. RAW is supported by NASA JWST grants NNX14AN10G and NAG5-12460.

A Starburst galaxies catalogs and selection criteria

In this appendix, details are given on how the list of SBGs considered here (Table 1) was obtained. For comparison, let us first summarize the approach and data in the AUG paper. The primary result there was obtained using the Fermi SBG catalog, but other data sets were also tested with results (i.e., a significant anisotropy) consistent with the primary analysis. Below the different SBGs sets are described briefly. They are:

- A selection of SBGs searched for in gamma-ray emission with Fermi-LAT [25]. In the search, a set of SBGs was compiled from a survey of the dense molecular gas tracer, HCN [33]. This HCN survey is statistically complete for northern galaxies (declination $\delta \geq -35^\circ$) with flux density at far-infrared (FIR) wavelength $\lambda = 100\mu$m of $S_{100\mu m} \geq 100$ Jy (corresponding to, approximately, a flux density $S_{60\mu\mathrm{m}} > 50$ Jy at $\lambda = 60\mu$m). However, the full SBGs set includes additional, fainter SBGs ($S_{60\mu\mathrm{m}} < 50$ Jy), which were used to establish the relationship between HCN luminosities and star formation rates over a wide range of FIR luminosities (see [33] for more details). Therefore, the full data set is not complete, and it does not fully satisfy the assumption of a uniformly sampled all-sky distribution (which is required by our method of analysis).

- The Fermi-LAT Third Source Catalog (3FGL) [26], from which the list of the 6 SBGs observed in gamma rays (NGC 253, M82, NGC 4945, NGC 1068, Circinus[5], NGC 2146) was obtained.

- the 2009 catalog by Becker et al. [27]. These authors use the FIR flux as a proxy for star-formation. Certain criteria were required for inclusion in the catalog, to ensure its completeness and to remove contamination from other astrophysical objects. They are:
  (1) a FIR flux density of $S_{60\mu\mathrm{m}} > 4$ Jy,
  (2) a radio flux density of $S_{1.4\mathrm{GHz}} > 20$ mJy,
  (3) a ratio of FIR to radio flux densities of $S_{60\mu\mathrm{m}}/S_{1.4\mathrm{GHz}} > 30$.
  (4) An additional constraint on the redshift of $z < 0.03$ (distance $D < 130$ Mpc), was placed to ensure that the SBGs were locally within the Super-Galactic plane [34, 35].
  The radio fluxes were extracted from the NRAO VLA Sky Survey (NVSS) [36], which is limited in declination to $\delta > -40^\circ$. Therefore, the Becker et al. compilation has a similar restriction in declination. It differs from Fermi SBGs set largely in its distance requirement and its all-sky completeness.

We took a fresh look at the problem of producing a sample of candidate SBGs as detailed and complete as possible. While the majority of IceCube neutrino events fall within the southern hemisphere, current SBGs catalogs are missing coverage in the crucial declinations of $\delta < -40^\circ$, due to a lack of radio surveys in that region (e.g. in HCN, or in the 1.4 GHz continuum). With the motivation to correct for this shortage, we turned to the Continuum HI Parkes All Sky Survey (CHIPASS) to extract the flux densities at $f = 1.4$ GHz for the brightest SBGs located at the most southern declinations. Essentially, the plan was to follow the same procedure that led to the Becker et al. catalog, with the additional 1.4 GHz measurements for sources with $S_{1.4\mathrm{GHz}} > 0.3$ Jy from the CHIPASS. The end goal here is to extend the galaxy sample that was used in AUG to include sources of $\delta < -40^\circ$.

[5]Circinus is not included in the list of SBGs that result from our selection criteria (discussed below, see Table 1). This might due to Circinus being located within 10° from the Galactic Plane, where FIR and radio obscuration is strong.

Here we briefly introduce the CHIPASS. It is a survey covering the Equatorial and Southern sky at $\delta < +25^\circ$ with the Parkes telescope, a single dish of 64 m in diameter located in Australia. The relatively poor angular resolution, $14.4'$ at 1.4 GHz, results in the image sensitivity being limited by confusion noise of $\sigma_c = 0.03$ Jy/beam. Hence, we expect our flux measurements to be somewhat beam-diluted, since the angular sizes of nearby galaxies are roughly $10'$ or less. However, the brightest galaxies, presumably contributing most to the neutrino and/or UHECR flux, would not be much affected by this dilution. Furthermore, by employing criterium (3) above, we strongly reduce the possibility of e.g. chance radio galaxies contaminating the radio flux of the sources.

As a first step towards creating a new set of SBGs, we used the IRAS Revised Bright Galaxy sample to identify the galaxies that are brightest at FIR frequencies. We imposed the same condition as in [27] on the FIR flux density, see criterion (1) above. In this way, a set of 195 SBGs (Set 1) was obtained.

For each candidate galaxy in Set 1, we reprojected the CHIPASS image [37] on a $15^\circ \times 15^\circ$ region centered at the object's coordinates. We then integrated the 1.4 GHz flux density within a circular aperture of width two times the beam full-width at half-maximum (i.e. $28.8'$). Instead of the criterion (2) above on the flux density, a stronger condition was required, namely $S_{1.4GHz} > 0.3$ Jy at $f = 1.4$ GHz, to match the one used in AUG. Finally, the conditions (3) and (4) as in [27] were imposed. The resulting list, Set 2, contained 13 SBGs. Finally, the union of Set 2 and the corresponding selection from the Becker et al. catalog was taken, producing the final list of 45 starburst galaxies shown in Table 1.

References

[1] K.-H. Kampert, A. A. Watson, and A. A. Watson, *Extensive Air Showers and Ultra High-Energy Cosmic Rays: A Historical Review*, *Eur. Phys. J.* **H37** (2012) 359–412, [arXiv:1207.4827].

[2] A. Letessier-Selvon and T. Stanev, *Ultrahigh Energy Cosmic Rays*, *Rev. Mod. Phys.* **83** (2011) 907–942, [arXiv:1103.0031].

[3] J. Linsley, *Evidence for a primary cosmic-ray particle with energy 10**20-eV*, *Phys. Rev. Lett.* **10** (1963) 146–148.

[4] **LIGO Scientific, Virgo** Collaboration, B. P. Abbott et al., *Observation of Gravitational Waves from a Binary Black Hole Merger*, *Phys. Rev. Lett.* **116** (2016), no. 6 061102, [arXiv:1602.03837].

[5] **IceCube** Collaboration, M. G. Aartsen et al., *First observation of PeV-energy neutrinos with IceCube*, *Phys. Rev. Lett.* **111** (2013) 021103, [arXiv:1304.5356].

[6] **Pierre Auger** Collaboration, A. Aab et al., *An Indication of anisotropy in arrival directions of ultra-high-energy cosmic rays through comparison to the flux pattern of extragalactic gamma-ray sources*, *Astrophys. J.* **853** (2018) L29, [arXiv:1801.06160].

[7] **Telescope Array** Collaboration, R. U. Abbasi et al., *Search for correlations between arrival directions of ultrahigh-energy cosmic rays detected by the Telescope Array experiment and a flux pattern from nearby starburst galaxies*, *Submitted to: Astrophys. J. Lett.* (2018) [arXiv:1809.01573].

[8] F. Capel and D. J. Mortlock, *Impact of using the ultra-high-energy cosmic ray arrival energies to constrain source associations*, arXiv:1811.06464.

[9] A. Loeb and E. Waxman, *The Cumulative background of high energy neutrinos from starburst galaxies*, *JCAP* **0605** (2006) 003, [astro-ph/0601695].

[10] I. Tamborra, S. Ando, and K. Murase, *Star-forming galaxies as the origin of diffuse high-energy backgrounds: Gamma-ray and neutrino connections, and implications for starburst history*, *JCAP* **1409** (2014) 043, [arXiv:1404.1189].

[11] L. A. Anchordoqui, T. C. Paul, L. H. M. da Silva, D. F. Torres, and B. J. Vlcek, *What IceCube data tell us about neutrino emission from star-forming galaxies (so far)*, *Phys. Rev.* **D89** (2014), no. 12 127304, [arXiv:1405.7648].

[12] K. Emig, C. Lunardini, and R. Windhorst, *Do high energy astrophysical neutrinos trace star formation?*, *JCAP* **1512** (2015) 029, [arXiv:1507.05711].

[13] R. Moharana and S. Razzaque, *Angular correlation between IceCube high-energy starting events and starburst sources*, *JCAP* **1612** (2016) 021, [arXiv:1606.04420].

[14] D. Hooper, T. Linden, and A. Vieregg, *Active Galactic Nuclei and the Origin of IceCube's Diffuse Neutrino Flux*, arXiv:1810.02823.

[15] K. Bechtol, M. Ahlers, M. Di Mauro, M. Ajello, and J. Vandenbroucke, *Evidence against star-forming galaxies as the dominant source of IceCube neutrinos*, *Astrophys. J.* **836** (2017), no. 1 47, [arXiv:1511.00688].

[16] T. Sudoh, T. Totani, and N. Kawanaka, *High-energy gamma-ray and neutrino production in star-forming galaxies across cosmic time: Difficulties in explaining the IceCube data*, *Publ. Astron. Soc. Jap.* **70** (2018), no. 3 Publications of the Astronomical Society of Japan, Volume 70, Issue 3, 1 June 2018, 49, https://doi.org/10.1093/pasj/psy039, [arXiv:1801.09683].

[17] X.-C. Chang and X.-Y. Wang, *The diffuse gamma-ray flux associated with sub-PeV/PeV neutrinos from starburst galaxies*, *Astrophys. J.* **793** (2014), no. 2 131, [arXiv:1406.1099].

[18] X.-C. Chang, R.-Y. Liu, and X.-Y. Wang, *Star-forming galaxies as the origin of the IceCube PeV neutrinos*, *Astrophys. J.* **805** (2015), no. 2 95, [arXiv:1412.8361].

[19] S. Chakraborty and I. Izaguirre, *Star-forming galaxies as the origin of IceCube neutrinos: Reconciliation with Fermi-LAT gamma rays*, arXiv:1607.03361.

[20] T. Linden, *Star-Forming Galaxies Significantly Contribute to the Isotropic Gamma-Ray Background*, *Phys. Rev.* **D96** (2017), no. 8 083001, [arXiv:1612.03175].

[21] **IceCube** Collaboration, M. G. Aartsen et al., *Observation of High-Energy Astrophysical Neutrinos in Three Years of IceCube Data*, *Phys. Rev. Lett.* **113** (2014) 101101, [arXiv:1405.5303].

[22] **ICECUBE** Collaboration, C. Kopper, W. Giang, and N. Kurahashi, *Observation of Astrophysical Neutrinos in Four Years of IceCube Data*, *PoS* **ICRC2015** (2016) 1081.

[23] **IceCube** Collaboration, C. Kopper, *Observation of Astrophysical Neutrinos in Six Years of IceCube Data*, *PoS* **ICRC2017** (2018) 981.

[24] **IceCube** Collaboration, M. G. Aartsen et al., *Observation and Characterization of a Cosmic Muon Neutrino Flux from the Northern Hemisphere using six years of IceCube data*, *Astrophys. J.* **833** (2016), no. 1 3, [arXiv:1607.08006].

[25] **Fermi-LAT** Collaboration, M. Ackermann et al., *GeV Observations of Star-forming Galaxies with Fermi LAT*, *Astrophys.J.* **755** (2012) 164, [arXiv:1206.1346].

[26] **Fermi-LAT** Collaboration, F. Acero et al., *Fermi Large Area Telescope Third Source Catalog*, *Astrophys. J. Suppl.* **218** (2015), no. 2 23, [arXiv:1501.02003].

[27] J. K. Becker, P. L. Biermann, J. Dreyer, and T. M. Kneiske, *Cosmic Rays VI - Starburst galaxies at multiwavelengths*, arXiv:0901.1775.

[28] **LSST** Collaboration, Z. Ivezic, J. A. Tyson, R. Allsman, J. Andrew, and R. Angel, *LSST: from Science Drivers to Reference Design and Anticipated Data Products*, arXiv:0805.2366.

[29] **EUCLID** Collaboration, R. Laureijs et al., *Euclid Definition Study Report*, arXiv:1110.3193.

[30] **WFIRST** Collaboration, O. Doré et al., *WFIRST Science Investigation Team "Cosmology with the High Latitude Survey" Annual Report 2017*, arXiv:1804.03628.

[31] D. B. Sanders, J. M. Mazzarella, D. C. Kim, J. A. Surace, and B. T. Soifer, *The iras revised bright galaxy sample (rbgs)*, *Astron. J.* **126** (2003) 1607, [astro-ph/0306263].

[32] D. G. Barnes, L. Staveley-Smith, W. J. G. de Blok, T. Oosterloo, I. M. Stewart, A. E. Wright, G. D. Banks, R. Bhathal, P. J. Boyce, M. R. Calabretta, M. J. Disney, M. J. Drinkwater, R. D. Ekers, K. C. Freeman, B. K. Gibson, A. J. Green, R. F. Haynes, P. te Lintel Hekkert, P. A. Henning, H. Jerjen, S. Juraszek, M. J. Kesteven, V. A. Kilborn, P. M. Knezek, B. Koribalski, R. C. Kraan-Korteweg, D. F. Malin, M. Marquarding, R. F. Minchin, J. R. Mould, R. M. Price, M. E. Putman, S. D. Ryder, E. M. Sadler, A. Schröder, F. Stootman, R. L. Webster, W. E. Wilson, and T. Ye, *The HI Parkes All Sky Survey: southern observations, calibration and robust imaging*, *Mon. Not. R. Astron. Soc.* **322** (Apr., 2001) 486–498.

[33] Y. Gao and P. M. Solomon, *HCN survey of normal spiral, IR - luminous and ultraluminous galaxies*, *Astrophys. J. Suppl.* **152** (2004) 63, [astro-ph/0310341].

[34] G. de Vaucouleurs, *Evidence for a local super galaxy*, *Astron. J.* **58** (Feb., 1953) 30.

[35] O. Lahav, B. X. Santiago, A. M. Webster, M. A. Strauss, M. Davis, A. Dressler, and J. P. Huchra, *The supergalactic plane revisited with the optical redshift survey*, astro-ph/9809343.

[36] J. J. Condon, W. D. Cotton, E. W. Greisen, Q. F. Yin, R. A. Perley, G. B. Taylor, and J. J. Broderick, *The NRAO VLA Sky survey*, *Astron. J.* **115** (1998) 1693–1716.

[37] M. R. Calabretta, L. Staveley-Smith, and D. G. Barnes, *A New 1.4GHz Radio Continuum Map of the Sky South of Declination +25 deg*, *Publ. Astron. Soc. Austral.* **31** (2014) 7, [arXiv:1310.2414].

Name	RA (J2000)	Dec (J2000)	Distance (Mpc)	$S_{60\,\mu\mathrm{m}}$ (Jy)	$S_{1.4\,\mathrm{GHz}}$ (Jy)
GC0055*	3.7664	-39.2077	3.1	77.0	0.37
NGC0157*	8.6917	-8.3981	21.92	17.93	0.31
NGC0253	11.8776	-25.2753	3.1	967.81	6.0
SMC*	13.2085	-72.7876	0.06	6688.9	1.26
NGC0660	25.7179	13.6358	12.33	65.52	0.37
NGC0839*	32.4288	-10.1842	51.1	11.67	0.37
NGC891	35.6392	42.3491	8.57	66.46	0.7
Maffei2	40.4795	59.6041	3.32	135.0	1.01
NGC1068	40.6645	-0.0020	13.7	196.37	4.85
NGC1097	41.6007	-30.2717	16.8	53.35	0.41
NGC1365	53.3839	-36.1408	17.93	94.31	0.53
IC342	56.7021	68.0961	4.6	180.8	2.25
NGC1482*	58.6658	-20.5019	25.09	33.36	0.31
NGC1569	67.7044	64.8479	4.6	54.36	0.4
NGC1672	71.4279	-59.2467	16.82	41.21	0.45
NGC1808	76.9319	-37.5228	12.61	105.55	0.5
LMC*	80.8938	-69.7561	0.05	82917.0	1.21
NGC2146	94.6571	78.3570	16.47	146.69	1.09
NGC2403	114.2140	65.6026	3.22	41.47	0.39
NGC2903	143.0460	21.5101	8.26	60.54	0.44
NGC3034(M82)	148.9680	69.6797	3.63	1480.42	7.29
NGC3079	150.4910	55.6797	18.19	50.67	0.82
NGC3256	156.9876	-43.9090	35.35	102.63	0.64
NGC3310	159.6910	53.5034	19.81	34.56	0.42
NGC3521*	166.4550	0.0375	6.84	49.19	0.35
NGC3628	170.0818	13.6037	10.04	54.8	0.47
NGC3627	170.0857	13.0005	10.04	66.31	0.46
NGC3690	172.1340	58.5622	47.74	113.05	0.66
NGC4038/9*	180.4873	-18.8984	21.54	45.16	0.54
NGC4254*	184.7063	14.4272	15.29	37.46	0.37
NGC4303	185.4808	4.4733	15.29	37.27	0.44
NGC4631	190.5330	32.5420	7.73	85.4	1.12
NGC4666	191.2860	-0.4619	12.82	37.11	0.43
NGC4818*	194.2083	-8.5272	9.37	20.12	0.45
NGC4945	196.3792	-49.4544	3.92	625.46	6.6
NGC5055(M63)	198.9560	42.0293	7.96	40.0	0.35
ESO173-G015*	201.8517	-57.4900	32.44	81.44	0.48
NGC5194(M51)	202.4700	47.1952	8.73	97.42	1.31
NGC5236(M83)	204.2532	-29.8586	3.6	265.84	2.44
NGC5643*	218.2197	-44.1990	13.86	23.48	0.36
UGC09913(Arp220)	233.7379	23.5028	79.9	104.09	0.32
NGC6240	253.2442	2.4008	103.86	22.94	0.65
NGC6946	308.7180	60.1539	5.32	129.78	1.4
NGC7331	339.2670	34.4156	14.71	45.0	0.37
NGC7582*	349.5925	-42.3719	21.29	52.2	0.68

Table 1. The starburst galaxies used in this work, with their Equatorial coordinates (in degrees) and their flux densities at 1.4 GHz and $60\mu m$. The flux extracted from CHIPASS has a maximum error of $\sim 20\%$. Asterisks mark the galaxies of our Set 2, which were not included in the AUG analysis. The four SBGs that contribute the most to the AUG anisotropy are marked in bold.